Manuscript submitted to: Volume, 1, 2013, 1-10.

AIMS's Materials Science DOI: 10.3934/matersci.2013.1.1

Received date 25 Sep 2013, Accepted date 20 Nov 2013, Published date 03 Dec 2013

Research article

Characterization of Chiral Carbonaceous Nanotubes Prepared from Four Coiled Tubular 4,4′-biphenylene-silica Nanoribbons

Shuwei Lin, Yitai Fu, Yunsen Sang, Yi Li, Baozong Li and Yonggang Yang*

Jiangsu Key Laboratory of Advanced Functional Polymer Design and Application, Department of Polymer Science and Engineering, College of Chemistry, Chemical Engineering and Materials Science, Soochow University, Suzhou 215123, P.R. China.

* **Corresponding author:** E-mail address: ygyang@suda.edu.cn (Y. Yang); Tel: +86 512 65880047; Fax: +86 512 65882052.

Abstract: Four dipeptides derived from phenylalanine were synthesized, which can self-assemble into twisted nanoribbon in deionized water. The handedness of the organic self-assemblies was controlled by the chirality of the phenylalanine at the terminals. Coiled 4,4′-biphenylene bridged polybissilsesquioxane tubular nanoribbons were prepared using the organic self-assemblies as the templates. The circular dichroism spectra indicated that the biphenylene rings preferred to twist in one-handedness within the walls of the samples. After carbonization and removal of silica, single-handed coiled carbonaceous tubular nanoribbons were obtained. The Raman spectra indicated that the carbon was amorphous. The diffuse reflectance circular dichroism spectra indicated the tubular carbonaceous nanoribbons exhibited optical activity.

Keywords: Self-assembly; Chirality; Nanostructures; Sol-gel growth; Carbonaceous materials

1. Introduction

With the development of carbon nanotubes, fullerene, and graphene, porous carbonaceous materials arouse much attention due to their varieties of potential applications [1,2]. Both the morphologies, pore architectures and crystallinity of the walls were controlled. For the carbons with chiral and helical structures, they are potentially applied for electromagnetic wave absorption and supaercapacitor electrode [3–12]. Although they can be prepared using a chemical vapor deposition method, it is hard to control their handedness [3–7]. For the single-walled carbon nanotubes, although they can be separated by chromatography and selective solubilization, the procedures are tedious [8–10]. It was reported recently that single-handed helical carbonaceous nanotubes can be

prepared by the carbonization of polypyrrole [11]. It is interesting to find that they exhibit optical activity.

During the last decade, the preparation and characterization of the single-handed helical polybissilsesquioxane nanofibers and nanotubes have been widely studied [12–17]. The helical polybissilsesquioxanes can be prepared through both external and self-templating approach. For the external templating approach, the self-assemblies of low-molecular-weight gelators (LMWGs) are usually used as the templates. After removing templates, mesoporous or tubular polysilsesquioxane nanofibers were obtained [12, 14–17]. The circular dichroism (CD) spectra indicated that the polysilsesquioxanes exhibit chirality at molecular level [17]. It was reported by us the single handed helical carbonaceous nanotubes can be prepared using the polysilsesquioxane nanotubes by carbonization and removal of silica [12]. The carbonaceous nanotubes also exhibit optical activity. Left-handed and right-handed helical nanotubes reflect opposite chiral circularly polarized light. However, the origin of the optical activity is still unclear. Therefore, to understand the structure/optical activity relationship, more helical carbonaceous nanotubes should be prepared. Herein, single-handed coiled tubular carbonaceous nanoribbons were prepared through a same approach. Their optical activity was studied using diffused reflectance CD (DRCD).

2. Materials and Method

2.1. Chemicals and reagents

4,4′-bis(triethoxysilyl)-1,1′-biphenyl (BTSB) was obtained from Suzhou Soochiral Sci & Tec. Co., Ltd. 3-Aminopropyltrimethoxysilane (APTMS) were purchased from the Aldrich Chem. Co., Ltd. Sodium hydroxide, ethanol and HF aqueous solution were purchased from Sinopharm Chemical Reagent Co., Ltd. The LMWGs were synthesized according to the literature (Fig. 1) [18,19].

2.2. General methods

FT-IR spectra were recorded using KBr pellets for solids on a Nicolet 6700 FT-IR spectrometer in the 4000–400 cm^{-1} range, with a resolution of 2.0 cm^{-1} and after accumulation of 32 scans. Elemental analyses were performed using a Perkin Elmer series II CHNS/O analyzer 2400. Transmission electron microscopy (TEM) images were obtained using an FEI TecnaiG220 at 200 kV. Field-emission scanning electron microscopy (FE-SEM) was performed using a Hitachi 4800 instrument at 3.0 kV. Small angle X-ray diffraction (SAXRD) pattern was obtained using an X′ Pert-Pro MPD X-ray diffractometer using Cu Kα radiation with a Ni filter (1.542 Å). The CD spectra were obtained using an AVIV 410 spectrophotometer with a 1.0 nm bandwidth, 1 scan and an averaging time of 0.1 s using a 0.1 mm cell at 25 ºC. DRCD and DRUV-vis spectra were obtained using a JASCO 815 spectrophotometer. The Raman spectra were taken using a Labram confocal microprobe Raman system. The sizes of the silt and pinhole were 100 and 400 μm, respectively. The Ar laser excitation wavelength was 514.5 nm, and largest laser power was 10 mW.

3. Synthesis

3.1. Characterization of the LMWGs

*Characterization of (L, L)-**3***. FT-IR (KBr, cm^{-1}): 3299 (ν_{N-H}, amide A), 1654 ($\nu_{C=O}$, amide I), 1533 (ν_{N-H}, amide II). ^{1}H-NMR (400 MHz, DMSO-d_6, TMS, 25 °C): δ = 0.85 (*t*, 3H; *J* = 6.6 Hz, –C$\underline{H_3}$CH$_2$), 1.06-1.24 (*m,* 24H; CH$_3$(C$\underline{H_2}$)$_{12}$CH$_2$), 1.38 (*t*, 2H; *J* = 7.4 Hz, –C$\underline{H_2}$CH$_2$CO), 2.04 (*t*, 2H, *J* = 6.8 Hz, –CH$_2$C$\underline{H_2}$CO), 2.66–2.76 (*m*, 2H; PhCHC$\underline{H_2}$COONa), 3.01–3.07 (*m*, 2H; CHC$\underline{H_2}$Ph), 4.43–4.51 (*m*, 1H; CONHC$\underline{H}$COONa), 4.66–4.70 (*m*, 1H; CONHC$\underline{H}$CONH), 7.10–7.23 (*br*, 10H, 2Ph), 8.00–8.05 (*m*, 1H, CON$\underline{H}$CHCOONa), 8.27 (*d*, 1H, *J* = 8.8 Hz, CON$\underline{H}$CHCONH). Elemental analysis for $C_{34}H_{49}N_2NaO_4$ calcd (%): C, 71.30; H, 8.62; N, 4.89. Found: C, 70.66; H, 8.94; N, 4.38.

*Characterization of (L, D)-**3***. FT-IR (KBr, cm^{-1}): 3295 (ν_{N-H}, amide A), 1650 (cm^{-1}, amide I), 1541 (ν_{N-H}, amide II). ^{1}H-NMR (400 MHz, DMSO-d_6, TMS, 25°C): δ = 0.85 (*t*, 3H; *J* = 6.6 Hz, C$\underline{H_3}$CH$_2$), 1.08-1.24 (*m,* 24H; CH$_3$(C$\underline{H_2}$)$_{12}$CH$_2$), 1.38 (*t*, 2H; *J* = 7.0 Hz, C$\underline{H_2}$CH$_2$CO), 2.04 (*t*, 2H, *J* = 7.2 Hz,CH$_2$C$\underline{H_2}$CO), 2.67-2.73 (*m*, 2H; PhCHC$\underline{H_2}$COONa), 3.02-3.08 (*m*, 2H; CHC$\underline{H_2}$Ph), 4.46-4.52 (*m*, 1H; CONHC$\underline{H}$COONa), 4.68-4.71 (*m*, 1H; CONHC$\underline{H}$CONH), 7.10-7.23 (*br*, 10H, 2Ph), 8.01-8.06 (*m*, 1H, CON$\underline{H}$CHCOONa), 8.28 (*d*, 1H, *J* = 8.4 Hz, CON$\underline{H}$CHCONH). Elemental analysis for $C_{34}H_{49}N_2NaO_4$ calcd (%): C, 71.30; H, 8.62; N, 4.89. Found: C, 70.08; H, 8.91; N, 4.58.

*Characterization of (D, L)-**3***. FT-IR (KBr, cm^{-1}): 3298 (ν_{N-H}, amide A), 1651 ($\nu_{C=O}$, amide I), 1534 (ν_{N-H}, amide II). ^{1}H-NMR (400 MHz, DMSO-d_6, TMS, 25 °C): δ = 0.85 (*t*, 3H; *J* = 6.6 Hz, –C$\underline{H_3}$CH$_2$), 1.07–1.24 (*m,* 24H; CH$_3$(C$\underline{H_2}$)$_{12}$CH$_2$), 1.38 (*t*, 2H; *J* = 7.2 Hz, –C$\underline{H_2}$CH$_2$CO), 2.04 (*t*, 2H, *J* = 6.8 Hz, –CH$_2$C$\underline{H_2}$CO), 2.66–2.73 (*m*, 2H; PhCHC$\underline{H_2}$COONa), 3.02–3.06 (*m*, 2H; CHC$\underline{H_2}$Ph), 4.47–4.53 (*m*, 1H; CONHC$\underline{H}$COONa), 4.72–4.76 (*m*, 1H; CONHC$\underline{H}$CONH), 7.09–7.22 (*br*, 10H, 2Ph), 8.02–8.07 (*m*, 1H, CON$\underline{H}$CHCOONa), 8.29 (*d*, 1H, *J* = 8.4 Hz, CON$\underline{H}$CHCONH). Elemental analysis for $C_{34}H_{49}N_2NaO_4$ calcd (%): C, 71.30; H, 8.62; N, 4.89. Found: C, 70.20; H, 8.87; N, 4.39.

*Characterization of (D, D)-**3***. FT-IR (KBr, cm^{-1}): 3296 (ν_{N-H}, amide A), 1652 ($\nu_{C=O}$, amide I), 1534 (ν_{N-H}, amide II). ^{1}H-NMR (400 MHz, DMSO-d_6, TMS, 25 °C): δ = 0.85 (*t*, 3H; *J* = 6.8 Hz, C$\underline{H_3}$CH$_2$), 1.07-1.24 (*m,* 24H; CH$_3$(C$\underline{H_2}$)$_{12}$CH$_2$), 1.38 (*t*, 2H; *J* = 7.4 Hz, C$\underline{H_2}$CH$_2$CO), 2.04 (*t*, 2H, *J* = 7.2 Hz, CH$_2$C$\underline{H_2}$CO), 2.66-2.73 (*m*, 2H; PhCHC$\underline{H_2}$COONa), 3.03-3.07 (*m*, 2H; CHC$\underline{H_2}$Ph), 4.46-4.52 (*m*, 1H; CONHC$\underline{H}$COONa), 4.65-4.69 (*m*, 1H; CONHC$\underline{H}$CONH), 7.08-7.23 (*br*, 10H, 2Ph), 8.00-8.04 (*m*, 1H, CON$\underline{H}$CHCOONa), 8.27 (*d*, 1H, *J* = 8.0 Hz, CON$\underline{H}$CHCONH). Elemental analysis for $C_{34}H_{49}N_2NaO_4$ calcd (%): C, 71.30; H, 8.62; N, 4.89. Found: C, 69.83; H, 9.01; N, 4.64.

3.2. Synthetic procedure for the 4,4'-biphenylene-silicas

A typical synthesis procedure for SLL was shown as following. Amphiphile (L, L)-**3** (20 mg, 0.16 mmol) was dissolved in a mixture of ethanol (2.2 mL) and deionized water (1.8 mL). Then, APTMS (10 μL) was added to the solution at 0 °C under stirring. Thirty seconds later, BTSB (30 μL) was added to the solution. The mixture was continuously stirred for 4.0 min. Then, stirring was stopped. The reaction mixture was kept at 0 °C for 24 h and then 80 °C for 3 days. Finally, the product was collected by filtration, extracted with a mixture of ethanol and hydrochloric acid and dried in air. The other sample SDL, SLD, and SDD were prepared using (D, L)-3, (L, D)-3, and (D, D)-3, respectively.

3.3. Synthetic procedure for the coiled carbonaceous tubular nanoribbons

The above obtained single-handed coiled 4,4′-biphenylene bridged polybissilsesquioxane tubular nanorribbons were carbonized at 900 °C for 4.0 h with a heating rate of 3.0 °C min^{-1} in Ar. Samples were obtained by cooling to room temperature naturally. The obtained single-handed helical carbon/silicas were immersed in 10 wt% aqueous HF for 4.0 h and then washed with deionized water. Samples were dried in vacuum at 40 ºC overnight. The samples were named as CLL, CDL, CLD, and CDD, according to the corresponding polybissilsesquioxanes.

4. Results and discussion

4.1. Characterization of gelators

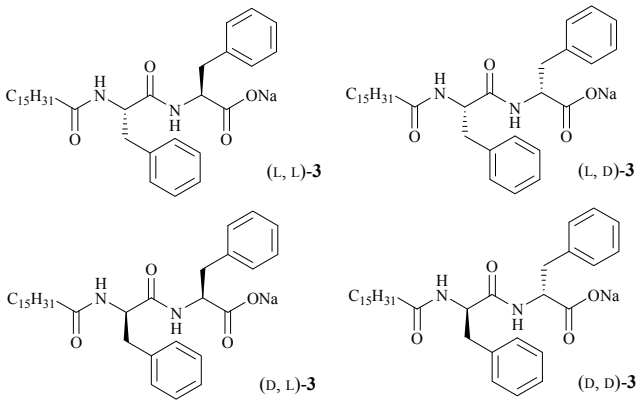

Figure 1. Molecular structures of the LMWGs.

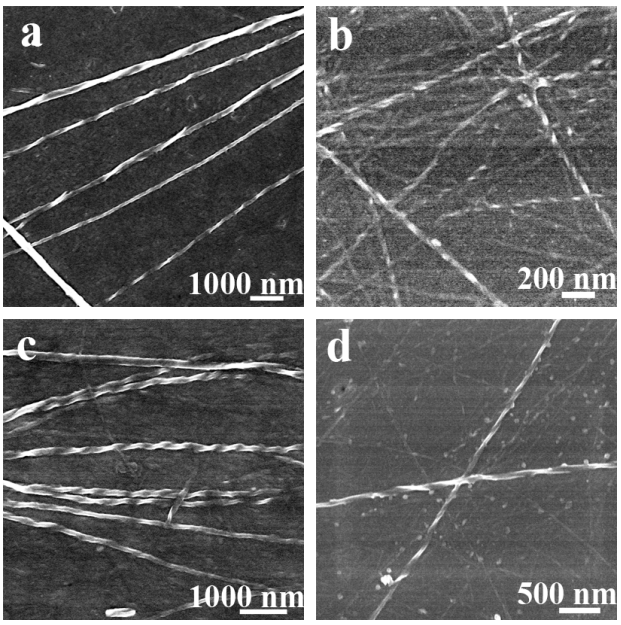

Figure 2. FE-SEM images of the xerogels of the LMWGs prepared at a concentration of 2.0 g L^{-1} in deionized water. (a) (L, L)-3; (b) (L, D)-3; (c) (D, L)-3; (d) (D, D)-3.

The molecular structures of the dipeptides are shown in Fig. 1. In order to study the chiral organization of the LMWGs in water, CD and UV spectra were taken at the concentration of 30.0 g L^{-1} using a 0.01 mm cell at 25 °C (Fig. S1, Supporting Information). The weak UV absorbance bands at 259 nm are originated from the phenyl group. The UV absorbance bands at 195 nm are mainly originated from the carbonyl groups. In the CD spectra, the $\lambda_{\theta=0}$ values appeared at 187–188 nm. The CD signs of (L, L)-**3** and (D, L)-**3** at about 260 nm were negative; and the CD signs of (L, D)-**3** and (D, D)-**3** at about 260 nm were positive, indicating the phenyl groups stacked in chiral in gel states. The handedness of the stacking of the phenyl groups was controlled by the chirality of the phenylalanine at the terminals. The CD signs of (L, L)-**3** at 220 and 197 nm were negative, indicating the carbonyl groups stacked in left-handedness. On the contrary, the carbonyl groups of (D, D)-**3** stacked in right-handedness. The CD signs of (L, D)-**3** at 220 and 202 nm were positive, indicating the carbonyl groups stacked in right-handedness. On the contrary, the carbonyl groups of (D, L)-**3** stacked in left-handedness. The CD spectra indicated that the chiral organization of the dipeptides was controlled by the chirality of the phenylalanines at the terminals. A similar phenomenon has been reported by us [18,19]. The hydrogen bondings among the amide groups and the electrostatic interactions among the carboxylate groups play important roles in the formation of the helical organic self-assemblies. FE-SEM images of the LMWGs prepared at a concentration of 2.0 g L^{-1} in deionized water are shown in Fig. 2. (L, L)-**3** and (D, L)-**3** self-assembled into left-handed twisted nanoribbons (Fig. 2a and c); and (L, D)-**3** and (D, D)-**3** self-assembled into right-handed twisted nanoribbons (Fig. 2b and d). The results are consistent with the CD data. These nanoribbons are 40–120 nm in width, 40 nm in thickness and 200 nm–2.5 μm in helical pitches. The helical pitch increased with increasing the width of the nanoribbons.

4.2. Characterization of 4,4'-biphenylene bridged polybissilsesquioxanes

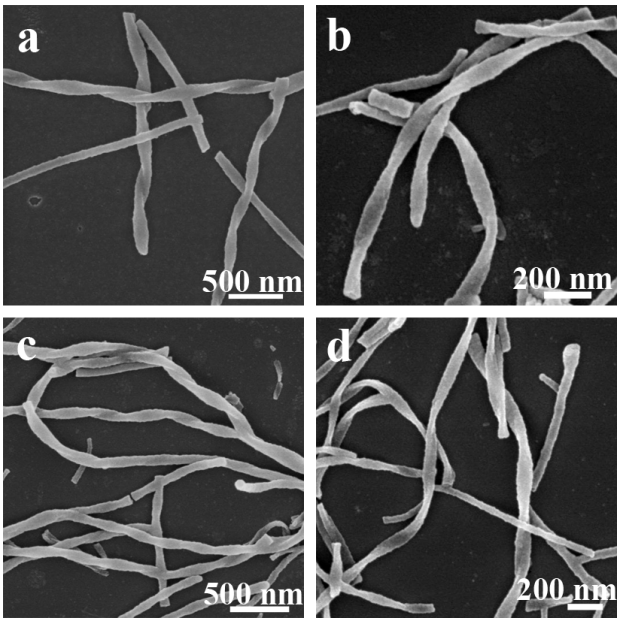

Figure 3. FE-SEM images of the samples. (a) SDD, (b) SLL, (c) SDL (D) SLD

The FE-SEM and TEM images images of the samples indicated that all of them are coiled tubular nanoribbons (Fig. 3 and S2, Supporting Information). SLL and SDL are left-handedness; and SDD and SLD are right-handedness. The handedness of them was controlled by their templates. Most of these nanotubes are about 100 nm in width, about 50 nm in thickness, and about 600 nm in helical pitch. The WAXRD patterns of these samples exhibit two peaks at 2θ of 7.28º and 14.66°, indicating a lamellar symmetry with a spacing of 12.2 Å (Fig. S3, Supporting Information) [15]. The intensity of the WAXRD peaks of these samples is weak. The addition of ethanol in the reaction mixtures is proposed to decrease the organization of the smallest repeat units. The formation of the coiled 4,4′-biphenylene bridged polybissilsesquioxane tubular nanoribbons should be as following [15,16]. With the addition of APTMS, the LMWGs and APTMS co-self-assemble into coiled nanoribbons. Then, 4,4′-biphenylene bridged polybissilsesquioxane oligomers adsorb on the surfaces of the organic co-self-assemblies through Si–O–Si covalent bonding. After polycondensation of the oligomers and removal of the LMWGs, tubular nanoribbons are obtained. Moreover, the helix is transferred from the organic self-assemblies (Fig. 2) to the polybissilsesquioxanes (Fig. 3).

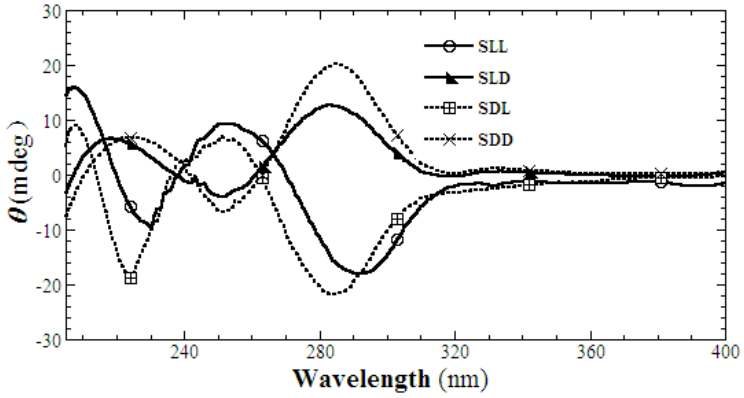

Figure 4. CD spectra of the 4,4′-biphenylene bridged polybissilsesquioxanes.

Biphenyl usually exhibits twisted conformations, where the twisted angles range from 30–45°. The handedness of the conformations can be revealed from their CD spectra [17]. For SLD and SDD, the first CD signals at 282–284 nm are positive, which originate from the electronic transition within the π systems of each biphenyl component (Fig. 4). The biphenyl component twists in a left-handed way. On the contrary, for SDL and SLL, the biphenyl component twists in a right-handed way. For SLL, the first CD signals shift to 291 nm. This shift was proposed to the decrease of the distance between the biphenyl components or the decrease of the distance between the carbon atoms of the biphenyl bond. Because these samples exhibit chirality at angstrom levels, they are potentially applied in asymmetric catalysis and enantioseparation. The results shown here also indicated that the handedness of the biphenyl component is not follow the handedness of the tubular nanoribbons at nano level. For example, although SLD exhibits right-handedness at nano level, the biphenyl component twists in left-handedness at angstrom level.

4.3. Characterization of the carbonaceous nanotubes

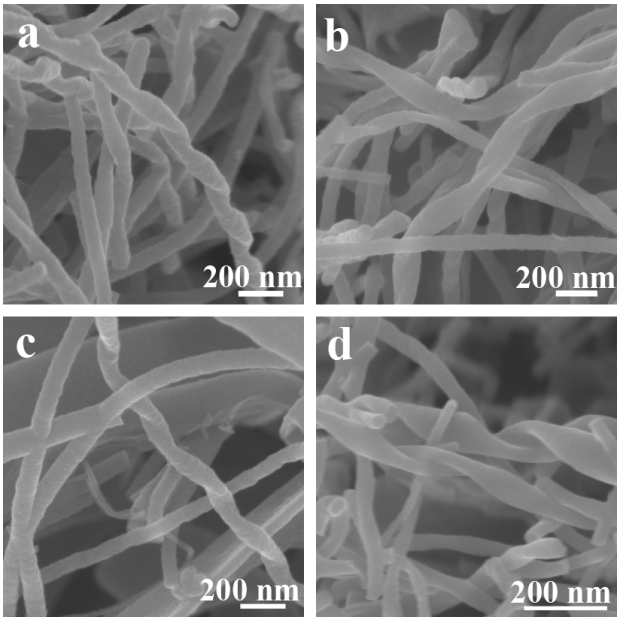

Figure 5. FE-SEM images of the samples. (a) CDD, (b) CLL, (c) CDL, (d) CLD.

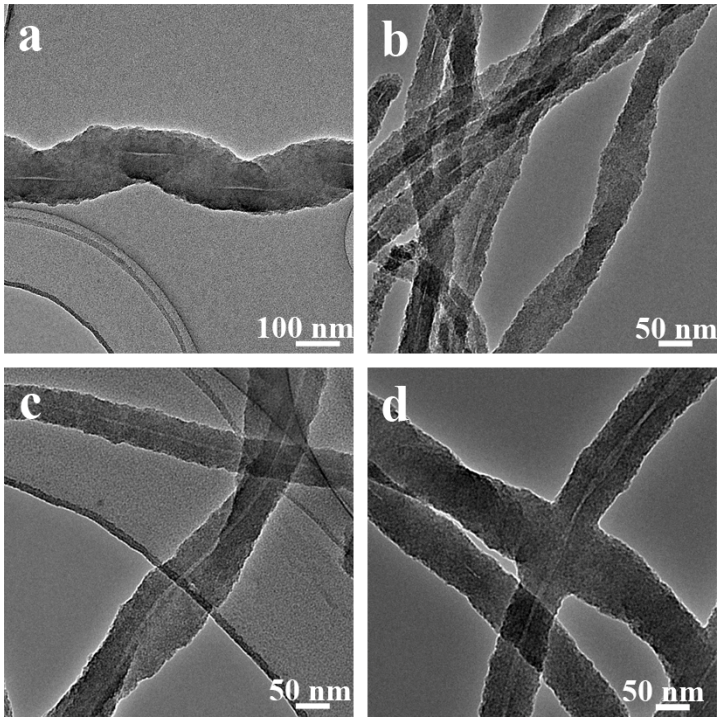

Figure 6. TEM images of the samples. (a) CDD, (b) CLL, (c) CDL, (d) CLD.

The FE-SEM and TEM images of the single-handed coiled carbonaceous tubular nanoribbons were shown in Fig. 5 and 6. Both the morphology and handedness were kept, similarly to the

polybissilsesquioxane tubular nanoribbons. The width, thickness and helical pitch are also similar as the polybissilsesquioxanes, indicating that the tubular nanoribbons did not shrink much after carbonization and removal of silica. Short and wormlike micropores were observed for the carbonaceous tubular nanoribbons, which should be formed due to the removal of silica (Fig. S4, Supporting Information). For the preparation of the polybissilsesquioxanes, APTMS was used as the co-structure directing agent. However, after carbonization, no nitrogen was identified from the energy dispersive spectrometer analysis. Therefore, the obtained samples are not N-doped carbonaceous materials. The TEM images are also indicated that the walls of the carbonaceous tubular nanoribbons are constructed by amorphous carbon.

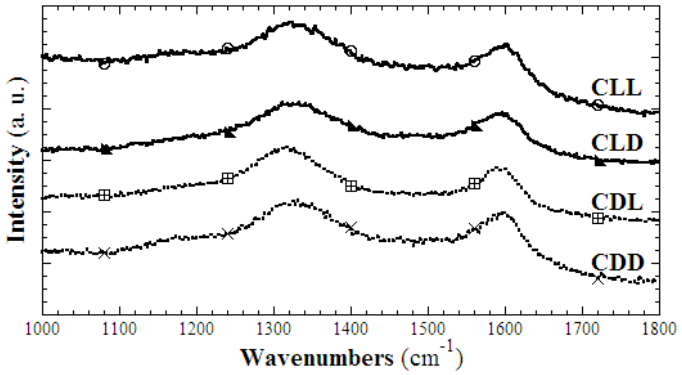

Figure 7. Raman spectra of the samples. (a) CDD, (b) CLL, (c) CDL, (d) CLD.

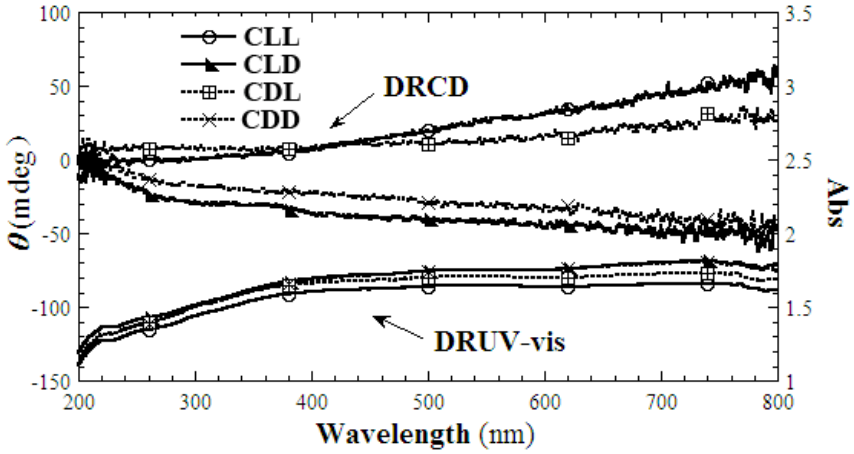

Figure 8. DRCD and DRUV-vis spectra of the carbonaceous tubular nanoribbons.

Raman spectra of carbonaceous tubular nanoribbons with 514.5 nm excitation are shown in Fig.7. These four spectra are nearly the same. The D bands were observed at about 1325 cm^{-1}. The I_G/I_D ratio indicated the crystalline sizes were less than several nanometers, which induced the G bands shifted to about 1598 nm [20]. DRCD and DRUV-vis spectra of the single-handed helical carbonaceous tubular nanoribbons are shown in Fig. 8. The carbonaceous samples show broad UV-vis absorbance bands from 200–800 nm. CLL and CDL exhibit positive DRCD signals at 200–800 nm. On the contrary, CLD and CDD exhibit negative DRCD signals at 200–800 nm. The

sign of the DRCD signals is follow the handedness of the carbonaceous tubular nanoribbons. It was proposed that the position of the DRCD signals was controlled by the helical pitch of the carbonaceous nanotubes. Our recent results indicated that single-handed helical carbonaceous nanotubes with helical pitches of 600–800 nm exhibited DRCD signals centered at about 380–400 nm. Herein, because some straight carbonaceous nanotubes exist in the samples, the intensity of the DRCD signals increases with increasing the wavelength from 200 to 800 nm (Fig. 5 and 6).

5. Conclusion

Four dipeptides derived from phenylalanine were synthesized, which can self-assemble into twisted nanoribbon in deionized water. The handedness of the organic self-assemblies was controlled by the chirality of the phenylalanine at the terminals. Coiled 4,4′-biphenylene bridged polybissilsesquioxane tubular nanoribbons were prepared using the organic self-assemblies as the templates. After carbonization and removal of silica, single-handed coiled carbonaceous tubular nanoribbons with micropores in the walls were obtained. The walls were constructed by amorphous carbon. The micropores were formed due to the removal of silica. These nanoribbons show broad DRCD singals at 200–800 nm.

Acknowledgments

This work was financially supported by the Natural Science Foundation of Jiangsu Province (Grant No. BK2011354) and the Priority Academic Program Development of Jiangsu High Education Institutions.

Conflict of interest

The authors declare that there are no conflicts of interest related to this study.

References

1. Meng Y, Gu D, Zhang F, Shi Y, Yang H, Li Z, Yu C, Tu B, Zhao D, (2005) *Angew. Chem. Int. Ed*. 44: 7053-7059.
2. Fang Y, Lv Y, Che R, Wu H, Zhang X, Gu D, Zheng G, Zhao D, (2013) *J. Am. Chem. Soc*. 135: 1524-1530.
3. Motojima S, Hoshiya S, Hishikawa Y, (2003) *Carbon* 41: 2658-2660.
4. Qin Y, Zhang Z, Cui Z, (2003) *Carbon* 41: 3072-3074.
5. Qin Y, Zhang Z, Cui Z, (2004) *Carbon* 42: 1917-1922.
6. Qin Y, Yu L, Wang Y, Li G, Cui Z, (2006) *Solid State Commun*. 138: 5-8.
7. Chen X, Yang S, Motojima S, Ichihara M, *Mater. Lett.* 2005, 59, 854-858.
8. Akazaki K, Toshimitsu F, Ozawa H, Fujigaya T, Nakashima N, (2012) *J. Am. Chem. Soc.* 134: 12700-12707.
9. Ozawa H, Fujigaya T, Niidome Y, Hotta N, Fujiki M, Nakashima N, (2011) *J. Am. Chem. Soc.* 133: 2651-2657.
10. Liu G, Yasumitsu T, Zhao L, Peng X, Wang F, Bauri A K, Aonuma S, Kimura T, Komatsu N, (2012) *Org. Biomol. Chem.* 10: 5830-5836.

11. Liu S, Duan Y, Feng X, Yang J, Che S, (2013) *Angew. Chem. Int. Ed.* 52: 6858-6862.
12. Zhang C, Li Y, Li B, Yang Y, (2013) *Chem. Asian J* .DOI: 10.1002/asia.201300798.
13. Moreau J J E, Vellutini L, Wong Chi Man M, Bied C, (2001) *J. Am. Chem. Soc.* 123: 1509-1510.
14. Wu X, Ji S, Li Y, Li B, Zhu X, Hanabusa K, Yang Y, (2009) *J. Am. Chem. Soc.* 131: 5986-5993.
15. Chen Y, Li Y, Chen Y, Liu X, Zhang M, Li B, Yang Y, (2009) *Chem. Commun.* 34: 5177-5179.
16. Li H, Li B, Chen Y, Zhang M, Wang S, Li Y, Yang Y, (2009) *Chin. J. Chem.* 27: 1860-1862.
17. Li B, Xu Z, Zhuang W, Chen Y, Wang S, Li Y, Wang M, Yang Y, (2011) *Chem. Commun.* 47: 11495-11497.
18. Fu Y, Li B, Huang Z, Li Y, Yang Y, (2013) *Langmuir* 29: 6013-6017.
19. Li Y, Li B, Fu Y, Lin S, Yang Y, (2013) *Langmuir* 29: 9721-9726.
20. Ferrari A C, Robertson *J,* (2000) *Phys. Rev.* 61: 14095-14107.

Supplementary The CD and UV spectra of the hydrogels; the TEM images and WAXRD patterns of the 4,4′-biphenylene bridged polybissilsesquioxanes; the TEM image of CLL.